Optics Communications 359 (2016) 393–398

Contents lists available at ScienceDirect

Optics Communications

journal homepage: www.elsevier.com/locate/optcom

Spatial and spectral selective characteristics of the plasmonic sensing using metallic nanoslit arrays

Caiwang Ge [a], Zhongyi Guo [a,b,*], Yongxuan Sun [b], Fei Shen [b], Yifei Tao [b], Jingran Zhang [b], Rongzhen Li [b], Linbao Luo [a]

[a] *School of Electronics Science and Applied Physics, Hefei University of Technology, Hefei 230009, China*
[b] *School of Computer and Information, Hefei University of Technology, Hefei 230009, China*

ARTICLE INFO

Article history:
Received 17 July 2015
Received in revised form
30 September 2015
Accepted 1 October 2015

Keywords:
Biosensing
Nanoslit arrays
Cavity mode
Surface plasmon polaritons (SPPs)
Spatial and frequency selective

ABSTRACT

A novel spatial and spectral selective plasmonic sensing based on the metal nanoslit arrays has been proposed and investigated theoretically, which shows a high performance in the multiplexing biomolecular detections. By properly tuning the geometric parameters of metal nanoslit arrays, the enhanced optical fields at different regions can be obtained selectively due to the excitation of SPP, cavity mode (CM), and their coupling effects. Simulation results show that the resonances of the metal nanoslit arrays at different spatial locations and different wavelengths can be achieved simultaneously. A relative bigger red-shift of 57 nm can be realized when a layer of biomolecular film is adsorbing at the slit walls, and the corresponding total intensity difference will be enhanced near 10 times compared to that at the top surface. In addition, when a BSA protein monolayer is adsorbing at slit walls with different slit widths, the corresponding wavelength shifts can reach to more than 80 nm by modulating the widths of the slit. The simulated results demonstrate that our designed metal nanoslit arrays can serve as a portable, low-cost biosensing with a high spatial and spectral selective performance.

1. Introduction

Surface plasmon resonance (SPR) sensing, a label-free and real-time sensing, has attracted extensive interests due to their wide applications in medical diagnostics, drug discovery, environmental sensing, and food safety monitoring [1–4]. Currently, commercially available sensors are dominated by the conventional propagating surface plasmon resonance (PSPR)-based systems, such as utilizing noble metal films or prisms [5,6]. Although the commercial PSPR-based sensors provide relatively high sensitivity, these systems require some complex and expensive equipments to couple and monitor lights, which hinders it's pervasive applications because it is difficult to be integrated into portable and low-cost microfluidic sensing devices [7]. Recently, the characteristics based on the extraordinary optical transmission (EOT) of the nanostructures has been utilized for biosensing applications [8]. In particular, nanoplasmonic sensors based on EOT through periodic nanoaperture arrays in metallic films provide relatively high sensitivities [9,10]. The resonance mechanisms behind EOT have been proved theoretically and experimentally, which mainly correspond to the SPP and cavity mode (CM) [11–14]. There are many applications by using SPP [15–17] and CM [18–19], but here we consider to combine the SPP and CM for plasmonic sensing. The resonant spectra of the SPP and CM sensitively vary with the structure parameters and the refractive index environment around the sensor.

EOT-based sensors have been widely discussed in some literatures. And many researchers have developed and optimized some sensors with different strategies, such as using suspended metal films [20], changing the shape of nanoapertures [21], employing more complex structures [22], and so forth. However, in most previous studies on the EOT-based sensors, they focus on optimizing the far-field sensor for the bulk refractive index changes. Just a few researchers have exploited alternative opportunities to develop the sensing performances by utilizing the plasmonics effects in enhanced near-field. For example, a novel important feature of the sensing mechanism with spatially selective sensing has been exploited by properly tuning the geometric parameters of a gold nanoslit array to tailor the spatial distribution of the enhanced optical field [10]. It is believable that the sensor will be more sensitive to refractive index changes in the close vicinity of the metallic structure, because the detected molecules lies in the confined and enhanced optical field. In addition, besides the spatial selective sensing of plasmon systems, there is another way to further improve sensor's performance by combining series of sensing unit cells with different resonant wavelengths for

---

[*] Corresponding author at: School of Electronics Science and Applied Physics, Hefei University of Technology, Hefei 230009, China.
E-mail addresses: guozhongyi@hfut.edu.cn (Z. Guo), luolb@hfut.edu.cn (L. Luo).

http://dx.doi.org/10.1016/j.optcom.2015.10.005

multiplexing detection [23]. Recently, by properly tuning the geometric parameters of a multi-layered metallic cross-shaped antennas, spatially and spectral selective plasmonic sensing in a multispectral plasmon resonance system has been demonstrated in theory [24], which has a superior performance in plasmonic biosensing, detection and imaging. However, it is limited by the complicated process for the corresponding structural fabrication.

In this letter, we present a simple structure of metal nanoslit arrays, which can realize the spatial and spectral selective plasmonic sensing for the biomolecules. We have investigated the sensing responses of the moleculars adsorbing at metal top surface and inside the nanoslit. And the simulated results show that the responses of the plasmonics sensing exhibit a multiband characteristics in the visible and near-infrared regions due to the excitations of SPP, CM and their coupling effects. By properly tuning the geometric parameters of the nanoslit arrays, the better sensing regions can be spatially transformed between the nanoslit walls and the top surface. Meanwhile, there also exist a spectral selective response for the different geometric conditions. These results show a higher performance in spatial and spectral selective sensing. And the surprisingly large peak shift of 57 nm can be obtained for a 5-nm-thick biomolecular film with a refractive index of 1.570. This novel spatial and spectral selective plasmonic sensing offers a new opportunity to optimize the performance of EOT-based biosensors and has a potential application in multiplexing biomolecular detections.

2. Structure and simulation

As depicted in Fig. 1, we consider a periodic array of subwavelength metallic nanoslits deposited on the polymethyl methacrylate (PMMA) substrate (with the depth of $d=200$ nm) as the samples. The period, the width and depth of the slit are indicated as P, W and D, respectively. In the following simulations, we set the environmental material on the top metal surface and inside the region of the nanoslits to be the air or water. The simulations are carried out by finite element method (FEM) to analyze the optical responses of the selected simulating unit cell. The refractive index of PMMA is 1.5 here, and the permittivity of the used silver is obtained from reference [25]. We set the periodic boundary conditions in both of the x and y directions. And the perfectly matching layers (PMLs) are utilized at the calculated region boundaries to reduce the influence of light reflection. The transverse magnetic (TM) polarized light is incident normally from the top of the structure.

3. Results and discussions

3.1. Optical properties of the nanoslit arrays

In general, there will be the resonant modes in the transmitted spectra, such as the cavity modes (CM) and the SPP modes, existing in the metallic nanoslits with suitable parameters (including the depth of the film, the period and the width of the nanoslits). When the depth of the deposited metal film is large enough, there will exist multi-order cavity modes in the transmitted spectra, which can be marked as CMi respectively, and i denote the orders of the CM in the nanoslits, corresponding to the number of nodes in the magnetic field distributions [26]. Firstly, we consider a thinner nanoslit arrays with $D=50$ nm, $P=500$ nm, and $W=26$ nm, respectively. As shown in Fig. 2, there is just one transmission peak in the corresponding transmitted spectrum, which can be attributed to the excitation of the SPP on the PMMA/metal interface. And it can be confirmed in the Fig. 3(a), where the magnetic field (|Hy|) at the resonance wavelength (707 nm) can demonstrate the typical SPP characteristics near the PMMA/metal interface clearly.

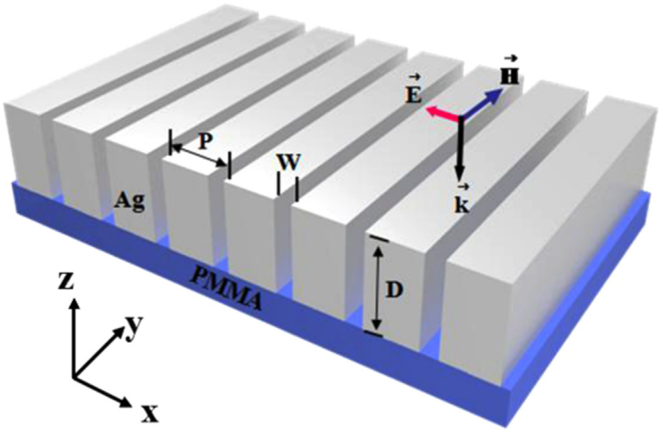

Fig. 1. Schematic of a metallic nanoslit arrays deposited on the PMMA, with the geometrical parameters (P, W and D), and the direction of the TM-polarized incident light.

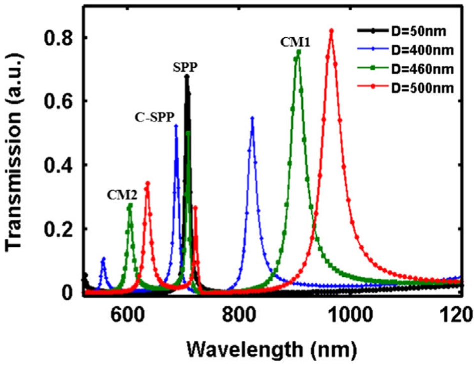

Fig. 2. Transmitted spectra of nanoslit arrays with different depths ($P=500$ nm, $W=26$ nm).

For a normal incidence, λ_{spp} can be described by following equation [27]:

$$\lambda_{spp}(n,\ i)=\frac{P}{i}Re\left\{\left(\frac{\varepsilon_m n^2}{\varepsilon_m+n^2}\right)^{1/2}\right\} \tag{1}$$

where n is the refractive index of environmental materials, i denotes the resonant order, P is the period of the nanoslit arrays and ε_m is the dielectric constant of the metal. The equation shows the SPP's resonant wavelength is sensitive to the variation of the environmental refractive index, which can be used as SPP based sensors. When the depths of the metal nanoslit (D) are increased from 400 nm to 500 nm, as shown in Fig. 2, there will be three transmission peaks in every transmitted spectrum, which have been marked as the CM1, C-SPP, and CM2 respectively. The peaks of CM1 and CM2 are the first and second orders of the cavity modes in nanoslits. As shown in Fig. 3(b) and (d), for the nanoslit with the depths of $D=460$ nm, under the normal incidences of 605 nm and 907 nm light separately, the number of nodes in the magnetic field distributions are 1 and 2 respectively, which agree well with theoretical expectations. As depicted in Fig. 3(c), for the nanoslit with the depths of 460 nm, under the normal incidence of 709 nm light, there coexist the CM and the SPP mode in the magnetic field distributions. Therefore, the C-SPP peaks can be attributed as the couplings of CMs in nanoslits and the excited SPP on the metal surface. From Fig. 2, we can observe that for the